Dendrochronologia 70 (2021) 125891

Contents lists available at ScienceDirect

Dendrochronologia

journal homepage: www.elsevier.com/locate/dendro

Wood anatomy and tree growth covary in riparian ash forests along climatic and ecological gradients

J. Julio Camarero [a,*], Michele Colangelo [a,b], Patricia M. Rodríguez-González [c], Ángela Sánchez-Miranda [d], Raúl Sánchez-Salguero [a,d], Filipe Campelo [e], Angelo Rita [f], Francesco Ripullone [b]

[a] Instituto Pirenaico de Ecología (IPE-CSIC), Avda. Montañana 1005, E-50192 Zaragoza, Spain
[b] Scuola di Scienze Agrarie, Forestali, Alimentari e Ambientali, Università della Basilicata, Viale dell'Ateneo Lucano 10, 85100 Potenza, Italy
[c] Forest Research Centre, School of Agriculture, University of Lisbon, Lisbon 1349-017, Portugal
[d] Departamento de Sistemas Físicos, Químicos y Naturales, Universidad Pablo de Olavide, 41013 Sevilla, Spain
[e] Centre for Functional Ecology, Department of Life Sciences, University of Coimbra, Calçada Martim de Freitas, 3000-456 Coimbra, Portugal
[f] Dipartimento di Agraria, Università di Napoli Federico II, via Università 100, 80055 Portici, Naples, Italy

ARTICLE INFO

Keywords:
Dendroecology
Floodplain forests
Fraxinus angustifolia
Hydraulic diameter
River hydrology

ABSTRACT

Riparian ash forests subjected to seasonal drought are among the most endangered ecosystems in Europe. They are threatened by climate warming causing aridification and by land-use changes modifying river flow. To assess the impacts of these two stress factors on riparian forests, we studied radial growth and xylem anatomical traits in five narrow-leaved ash (*Fraxinus angustifolia*) stands across wide climatic and ecological gradients from northern Italy to southern Portugal. Radial growth rates and earlywood hydraulic diameter (*Dh*) were directly correlated, whilst earlywood vessel density and growth rates were inversely associated. Ash growth positively responded to precipitation. Higher and lower rates of growth increase in response to precipitation were found in dry (annual precipitation 357–750 mm, annual water balance −39 to −48 mm) and wet (annual precipitation 1030 mm, annual water balance 27 mm) sites, respectively. Wet conditions in autumn and winter of the year prior to tree-ring formation lead to larger *Dh* values, except in the wet site where warmer conditions from prior autumn to current spring were positively associated to wider vessels. Growth was also enhanced by a higher river flow, reflecting higher soil moisture due to elevated groundwater table levels. Peaks in river flow from late winter to early spring increased *Dh* in dry-continental sites. Growth and potential hydraulic conductivity in drought-prone riparian ash forests are differently impacted by climate variability and river flow depending on site and hydrological conditions. Nevertheless, covariation between radial growth and the earlywood vessel diameter was found, regardless of site specific differences. Wood production and hydraulic conductivity are coordinated through the production of large earlywood vessels which may allow reaching higher growth rates.

1. Introduction

Riparian forests are among the most threatened wetland habitats because they have been severely impacted by climate warming, land-use changes and biotic stressors such as pathogens and invasive species (Dufour et al., 2018; Stella and Bendix, 2019). In seasonally dry regions such as the Mediterranean Basin rising temperatures increase the atmospheric water demand exacerbating aridification, which could reduce riparian forest productivity (Gomes Marques et al., 2018). However, assessments on the impacts of extreme climatic events such as droughts on the growth and wood anatomy of Mediterranean riparian forests are lacking. The importance of studying these climate impacts on growth of these riparian forests is due to their menaced conservation status and their elevated productivity which may be reduced by recurrent droughts (Rodríguez-González et al., 2021).

Human land-use changes have negatively influenced floodplain

* Corresponding author.
E-mail addresses: jjcamarero@ipe.csic.es (J.J. Camarero), michelecolangelo3@gmail.com (M. Colangelo), patri@isa.ulisboa.pt (P.M. Rodríguez-González), asanchezmirandam@gmail.com (Á. Sánchez-Miranda), rsanchez@upo.es (R. Sánchez-Salguero), fcampelo@uc.pt (F. Campelo), angelo.rita@unina.it (A. Rita), francesco.ripullone@unibas.it (F. Ripullone).

https://doi.org/10.1016/j.dendro.2021.125891
Received 6 May 2021; Received in revised form 17 September 2021; Accepted 26 September 2021
Available online 29 September 2021

forests by modifying hydrological regimes and fluvial processes through dam and dike building, expanding agricultural lands and fragmenting riparian stands, and contributing to the spread of tree pathogens (Rodríguez-González et al., 2010, 2014; Valor et al., 2020; European Environment Agency EEA, 2015). Therefore, analysis across wide geographic and climatic gradients can provide a spatial analogy on how Mediterranean riparian forests will respond to climate warming, extreme climatic events and altered river flow.

Climatic (high atmospheric water demand due to dry-warm conditions) and hydrological (reduced soil moisture levels due to declines in water table depth) droughts reduce the water available to trees and decrease riparian Mediterranean forest growth productivity (Stella et al., 2013a, 2013b; Gomes Marques et al., 2018). However, functional approximations to reconstruct changes in proxies of productivity and hydraulic conductivity, such as radial growth and vessel lumen area or diameter, are lacking. Furthermore, growth and anatomy could be coordinated to enhance wood production and water transport, but this has not been tested in riparian species under field conditions.

In Mediterranean riparian forests, non-phreatophytic species with shallow roots such as the narrow-leaved ash (*Fraxinus angustifolia* Vahl) are expected to be less coupled to changes in streamflow and water table depth than phreatophytes such as poplar (Scott et al., 1999; Andersen, 2016; Schook et al., 2020). Ash species inhabit sites with shallow soil water pools making them more coupled to climate than to hydrological variability, i.e., they should be sensitive to climatic drought (Dufour and Piégay, 2008; Singer et al., 2013). In the Mediterranean Basin, narrow-leaved ash appears in floodplains or in mountain sites with moist soils (Rodríguez-González et al., 2008; Caudullo and Houston Durrant, 2016). To evaluate its sensitivity to hydroclimate, a quantification of radial-growth and wood-anatomical responses to temperature, precipitation and river flow in Mediterranean riparian ash stands is necessary. Radial growth is a proxy of long-term carbon uptake and storage in woody compartments and earlywood anatomy is a surrogate of tree hydraulic functioning (Fonti et al., 2010). Such complementary information is relevant for promoting a sustainable management of riparian forests and water resources affected by drought (Gomes Marques et al., 2018). These threatened ecosystems could become more vulnerable if the frequency of severe droughts increases and river flow decreases (Stella and Bendix, 2019; Rodríguez-González et al., 2021).

Ash species have been investigated by ecophysiologists, wood anatomists and dendroecologists because their big earlywood vessels provide a suitable system to quantify xylem vulnerability to drought- or frost-induced cavitation and how this affects hydraulics, gas exchange and growth (e.g., Utsumi et al., 1999). For instance, leaf hydraulic conductance and gas exchange rates in ash species were coupled with hydraulic conductivity and water availability (Cochard et al., 1997; Gortan et al., 2009). Other studies measured earlywood vessel transversal lumen area and density looking for climate signals in wood anatomical traits (Tardif, 1996; Zhu et al., 2020), but they were mainly carried out in cool wet regions where drought is rare (Klesse et al., 2020). In central and northern Europe the loss of productivity observed in riparian common ash (*Fraxinus excelsior* L.) forests has been linked to growth decline and elevated canopy dieback and mortality rates triggered by pathogens (Enderle et al., 2019; Hultberg et al., 2020; Klesse et al., 2020). Climate warming and pathogens could favor the long-term replacement of common ash by narrow-leaved ash in transitional areas of central Europe, but this forecast should be supported by analyses quantifying the impact of climate and river flow on growth and wood anatomy.

Here we study how radial growth and earlywood anatomy are related to climate variables and river flow in Mediterranean narrow-leaved ash (hereafter ash) populations across geographical and environmental gradients spanning different hydrologic regimes. We considered a wet site in northern Italy having a positive annual water balance, and four sites with negative water balances, two dry-continental sites located in north-eastern Spain and two dry-warm sites situated in south-western Iberia (Table 1). Xylogenesis studies have showed that climatic conditions during the preceding late winter and early spring, before vessel enlargement, determine the onset of cambial activity (Funada and Catesson, 1991; Gričar et al., 2020). Therefore, we expect that: earlywood vessel lumen area is related to previous winter climate conditions, particularly temperature in the wettest-coolest sites. We also hypothesize that vessel lumen area responds to river flow peaks recharging soil moisture pools before or during the early phases of vessel enlargement. Lastly, we hypothesize that the growth rate is coordinated with earlywood anatomy and such rate depends on precipitation in the warmest and driest sites. Testing these ideas is important to forecast the productivity and improve the conservation of Mediterranean riparian forests.

2. Materials and methods

2.1. Study sites

The five study sites were chosen to cover different geographical (latitude 37º–45º N, longitude 8º 30′ W–8º 30′ E, elevation 69–257 m), and climatic conditions (mean annual temperature 13–18 ºC, annual precipitation 357–1030 mm, annual water balance −68 to 27 mm) across the ash distribution area (Fig. 1a, Table 1).

Two sites were located in the Middle Ebro Basin (north-eastern Spain), where the river flows over the main plain with a low slope and forms meandering channels (Ollero, 2007). The Ebro basin covers 85, 362 km^2 and is the third largest basin in surface of the Mediterranean Basin. A mature, little disturbed floodplain forest was sampled near Tudela town ("Soto de la Remonta") and a slightly disturbed site was sampled near Zaragoza city ("Soto de Partinchas"), which was affected by dikes construction in the 1950–1960s (Ayerra, 1988; Ollero, 1990). These reservoirs profoundly altered the Ebro river regime, reducing the higher winter flows and rising water level in summer (Frutos et al., 2004). River flow peaks from January to April (see Fig. S1). Climate in this area is semi-arid Mediterranean continental. The coldest and warmest months are January (means of 5.4–5.6 ºC) and July (means of 22.7–23.6 ºC), respectively. Summer drought lasts from June to September. The substrates develop on marl and gypsum substrates producing basic, loamy-sandy soils. These forests are dominated by tamarisks (*Tamarix* spp.), white willow (*Salix alba* L.) and silver poplar (*Populus alba* L.) situated near the river bank, black poplar (*Populus nigra* L.) located in the transition zone, and ash with scattered elm trees (*Ulmus minor* Mill.) forming mature floodplain forests.

Table 1
Sites' geographical and climatic characteristics. The last two columns show the climatic water balance or difference between precipitation and potential evapotranspiration (P–PET).

Site	Latitude (N)	Longitude	Elevation (m a.s.l.)	Mean annual temperature (ºC)	Total annual precipitation (mm)	Annual P –PET (mm)	Summer P –PET (mm)
Odelouca	37º 14′	8º 30′ W	120	16.9	750	−39.38	−141.50
Doñana	37º 06′	6º 39′ W	69	18.1	549	−67.92	−179.96
Zaragoza	41º 42′	0º 56′ W	205	14.7	357	−60.25	−148.79
Tudela	42º 07′	1º 35′ W	257	13.9	485	−47.68	−130.83
Ticino	45º 26′	8º 50′ E	202	12.6	1030	27.50	−36.75

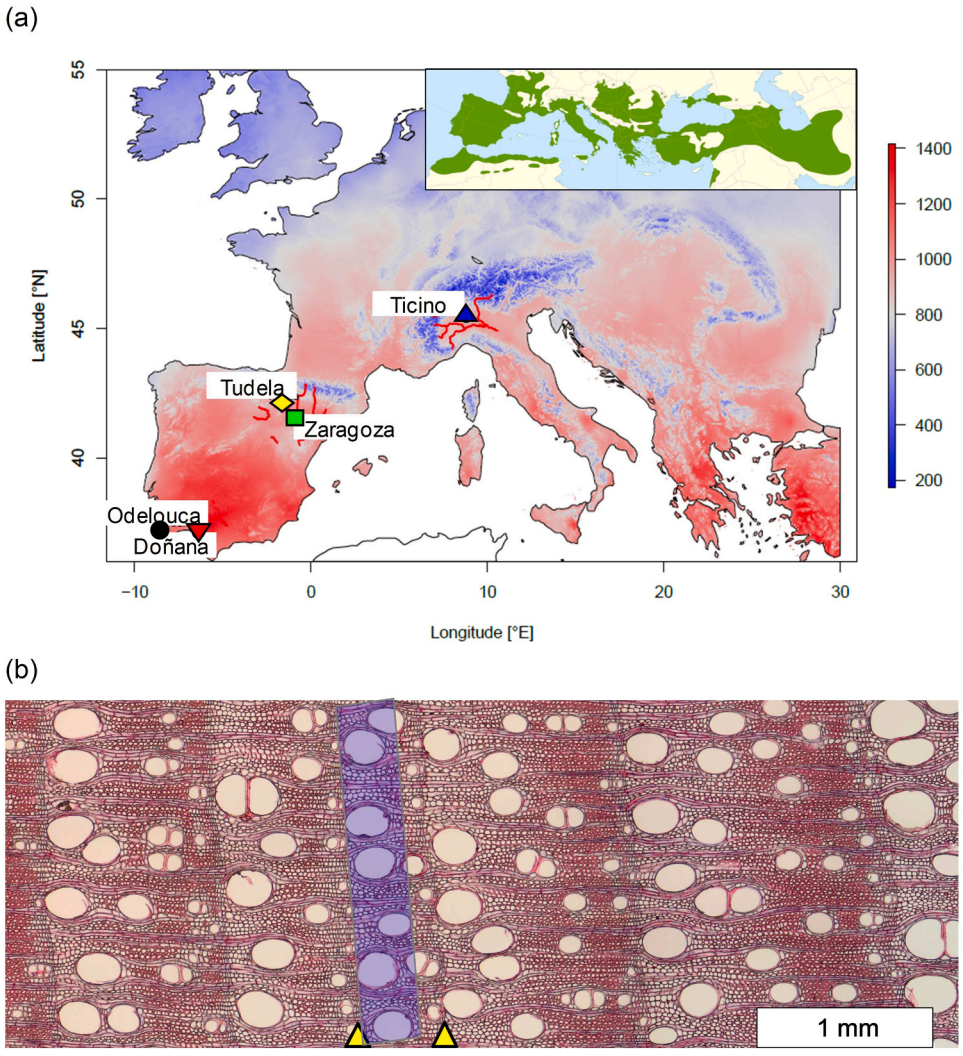

Fig. 1. (a) Map with the five ash sites and annual potential evapotranspiration in Europe (background and color scale). The river basins of the sampled ash stands are indicated with red, thick lines. The inset map shows the distribution of narrow-leaved ash (*Fraxinus angustifolia*) in green, according to Caudullo et al. (2017). (b) Wood cross-section of a narrow-leaved ash tree sampled near the Tudela site showing the narrow 2012 ring (the rings is delimited by the upwards yellow triangles and its earlywood is delimited by the blue box; the bark is located towards the right side of the image). This narrow ring was produced in response to a severe climatic and hydrological drought reducing the Ebro river flow in March (see Fig. S1c). (For interpretation of the references to color in this figure legend, the reader is referred to the web version of this article.)

The Doñana floodplain forest (La Rocina) is located in a stream feeding from its western part the "Doñana National Park" marshes (southwestern Spain). The stream collects runoff and groundwater along a sandy catchment of around 400 km^2 in a Guadalquivir river sub-basin (Manzano et al., 2005). This site has a Mediterranean sub-humid climate with rainy autumns and winters, hot and dry summers and mild winters. The mean annual precipitation is 549 mm and the mean annual temperature is 18.1 ºC, with January (4.6 ºC) and July (32.6 ºC) being the coldest and warmest months, respectively. Floods peak in late winter. Clay and silt geological substrates predominate. This floodplain forest is dominated by willow (*Salix atrocinerea* Brot.) and ash (Rodríguez-González et al., 2017).

The Odelouca site is situated in the Odelouca basin (southern Portugal), which has 511 km^2 of drainage area and 92 km of slow-running streams, with a free-flowing Mediterranean flooding regime. Mean annual precipitation is 750 mm, mostly concentrated from October to April, and the dry period lasts from June to September. The monthly temperatures range between 11.6 ºC (January) and 23.1 ºC (August). The main substrates are clay shales, greywacke and sandstones. Forests are dominated by ash, willow (*Salix salviifolia* Brot.), tamarisk (*Tamarix africana* Poir), oleander (*Nerium oleander* L.) and black alder (*Alnus glutinosa* [L.] Gaertn.) (Rodríguez-González et al., 2014; Gomes Marques et al., 2018).

The Ticino study site is part of the upper Po sub-basin in northern Italy and has been regulated for the past 60 years (Colangelo et al., 2018). Climate is temperate and humid with annual precipitation of 1030 mm, with the highest and lowest rainfall values recorded in October (122 mm) and January (59 mm), respectively. The mean annual temperature is 12.6 ºC, with January (0.8 °C) and July (24.6 °C) as the coldest and warmest months, respectively. The upper Po plain shallow aquifer, which is constituted by gravel and sand deposits over discontinuous clay layers, is located at least 50 m below the land surface. The substrate is dominated by sandy loam soils. In the study site, mixed stands of oaks (*Quercus robur* L. and *Quercus petraea* Liebl.), *A. glutinosa* and *U. minor* abound, whilst some stands are dominated by the exotic black locust (*Robinia pseudoacacia* L.) (Colangelo et al., 2018).

2.2. Climate, drought and hydrological data

To obtain homogenized long-term series of monthly climatic data (mean temperature, total precipitation) we used the 0.25º-gridded E-OBS dataset ver. 15.0 (Cornes et al., 2018). For each study site, we downloaded the corresponding series from the nearest 0.25º grid point. To assess site dryness we calculated the climatic water balance or difference between precipitation and potential evapotranspiration (P–PET). Evapotranspiration was calculated using the Penman-Monteith equation and obtained from the 30-sec gridded dataset of Trabucco and Zomer (2019). We also calculated the site precipitation for the hydrological year, from prior October to current September.

Long and continuous monthly hydrological data (river flow) were

only available for the two sites located in the Ebro basin, where the role of hydrology was evaluated. We obtained flow data for the period 1970–2016 from the Spanish National Flow and Discharge Database (Centro de Estudios y Experimentación de Obras Públicas, https://ceh.cedex.es). Flow data were obtained from two gauging stations located in Castejón (42º 11′ N, 1º 41′ W, 260 m a.s.l.) and Santiago (41º 39′ N, 0º 53′ W, 201 m a.s.l.) bridges and located 10.4 km and 6.2 km upstream and downstream from Tudela and Zaragoza sites, respectively. Older flow data (1915–1939) from Zaragoza were also used to illustrate how the regulation of the Ebro river after reservoir building changed the natural flow regime (Fig. S1a).

2.3. Field sampling and dendrochronological data

Tree-ring data and earlywood anatomy were quantified for different periods because of logistic constraints. Sampling was done from 2014 to 2017 in all sites, excepting Odelouca where sampling was done in 2009 when trees were felled and a reservoir was built. Field sampling included the measurement of tree diameter at breast height (Dbh, 1.3 m) using tapes or calipers and coring of dominant, visually healthy trees using 5-mm wide Pressler increment borers. We selected and sampled from 12 to 17 mature, dominant and apparently healthy trees of similar height per site (Table 2). Two increment cores per tree were sampled at 1.3 m. Tree rings were visually cross-dated and tree-ring widths were measured to the nearest 0.01 mm using a binocular microscope coupled to a computer with the LINTAB-TSAP package (Rinntech, Heidelberg, Germany). Tree age at 1.3 m was estimated such as the maximum number of rings counted in the radii of each tree and considering only those cores showing the pith or curved innermost rings. In samples without pith, we estimated the number of missing rings by fitting template of concentric circles to the innermost, curved rings so as to establish relationships between the estimated distance up to the theoretical pith (assuming concentric growth) and the number of missing rings. These regressions between distance and number of rings were built with samples containing the pith.

The largest stem diameters at 1.3 m (36–46 cm) and radial-growth rates (3.21–3.97 mm) were found in Odelouca and Ticino, and the lowest ones in Doñana (diameter 30 cm, tree-ring width 2.18 mm). Trees were older in Odelouca and Doñana sites (61 years on average) than in the other sites (52 years on average) (Table 2).

2.4. Tree-ring width data processing

The COFECHA program was used to evaluate the visual cross-dating of tree-ring series (Holmes, 1983). We developed site-specific mean series of tree-ring width (TRW; Fig. S2a) or ring-width indices (RWI) using the *dplR* (Bunn, 2010; Bunn et al., 2018) and *detrendeR* R packages (Campelo et al., 2012). We fitted a cubic smoothing spline with a 50% frequency cutoff at 30 years to each tree-ring width series and obtained RWIs by dividing observed by fitted TRW values (Fritts, 1976). Then, auto-regressive models were selected by minimizing the Akaike Information Criterion (AIC) and applied to each RWI series. The resulting pre-whitened or residual series or chronologies were averaged using bi-weight robust means to compute five site chronologies (Fig. S2b). To determine the best-replicated period we calculated the Expressed Population Signal (EPS), which allows assessing how similar the chronologies are to an infinitely replicated chronology (Wigley et al., 1984). All RWI chronologies were adequately replicated since 1970 with EPS > 0.85.

2.5. Earlywood anatomy data

We selected five trees per site and one radius per tree to perform anatomical analyses of ash earlywood. Selected trees were those showing the highest correlation between their RWI series and the mean site series. Wood anatomy was analyzed for the common 1990–2009 period (see Table 2). Wood samples were transversally cut using a sledge core microtome (Gärtner and Nievergelt, 2010). Transversal wood sections (thickness of 15–20 μm) were prepared from each core tree by dividing it into 2-cm long pieces. Samples were stained with safranin (1%) and astra blue (2%) and images were captured at 20–40x magnification using a light microscope (Olympus BH2). Earlywood (hereafter EW) vessels were considered those with lumen diameters larger than 50 μm and located in the first half of the ring along the radial direction (see Fig. 1b). Radial EW vessel diameters and vessel areas were measured in a window of 4 mm (core width) using the ImageJ software for image analysis (Schneider et al., 2012).

2.6. Processing earlywood anatomy data

Xylem anatomical changes depend not only on environmental conditions but also on adjustments to tree ontogeny as shown by the universal relationship between plant height and vessel diameter (e.g., Olson et al., 2018). We considered these ontogenetic trends by sampling mature and dominant trees, by avoiding juvenile rings with small EW vessels, and by averaging series from trees of similar size and age (Table 2).

We calculated the percent area occupied by vessels and vessel density (*VD*). We also calculated the hydraulic diameter (*Dh*) for all EW vessels measured in each ring as $Dh = \sum d^5 / \sum d^4$, where d is the diameter of each EW vessel (Sperry et al., 1994). We also obtained the vulnerability index (*VI*), which was defined by Carlquist (1977) as the ratio between vessel diameter and vessel density (i.e., $VI = Dh/VD$), and provides an indication of the plant to withstand drought- or frost-induced xylem cavitation (Scholz et al., 2013). According to Carlquist (1977), *VI* values approaching 3.0 indicate mesomorphy (wood features adapted to mesic habitats such as big lumen areas, low vessel density or thin cell walls, among others), whereas *VI* values approaching 1.0 correspond to xeromorphy (wood features adapted to xeric habitats such as small lumen areas, high vessel density or thick cell walls, among others).

Only the EW vessel chronologies from Zaragoza showed EPS > 0.85. The largest and lowest *Dh* values were found in Ticino (0.304 mm) and Doñana (0.225 mm), respectively (Fig. 2). Vessel density peaked in Tudela (11 vessels mm^{-2}) and Doñana (10 vessels mm^{-2}). The *VI* was highest in Ticino and Zaragoza (2.5–2.7) and lowest in Tudela and Doñana (1.8–1.9).

Table 2
Mean values of growth rates and earlywood anatomical data with their standard errors. Data correspond to the 1990–2016 period for all sites excepting Doñana (1990–2014) and Odelouca (1990–2009). Different letters indicate significant ($p < 0.05$) differences between sites based on Mann-Whitney tests.

Site	No. trees (No. cores)	Dbh (cm)	Age at 1.3 m (years)	Best replicated period	Tree-ring width (mm)	*Dh* (mm)	Vessel density (No. mm^{-2})	Vulnerability Index
Odelouca	12 (24)	46.0 ± 3.0b	62 ± 13b	1953–2009	3.97 ± 0.91b	0.250 ± 0.002b	9.02 ± 0.19a	2.28 ± 0.52b
Doñana	12 (23)	30.0 ± 1.2a	61 ± 12b	1947–2014	2.18 ± 0.41a	0.225 ± 0.002a	9.98 ± 0.18b	1.84 ± 0.51a
Zaragoza	14 (28)	34.0 ± 1.2a	46 ± 3a	1969–2016	2.85 ± 0.55ab	0.255 ± 0.003b	8.91 ± 0.20a	2.50 ± 0.84 bc
Tudela	17 (26)	31.0 ± 2.0a	47 ± 12a	1970–2016	2.77 ± 0.43ab	0.250 ± 0.002b	10.82 ± 0.27c	1.95 ± 0.59a
Ticino	16 (23)	36.0 ± 1.4a	59 ± 14a	1969–2017	3.21 ± 0.74b	0.304 ± 0.004c	9.11 ± 0.11a	2.69 ± 0.48c

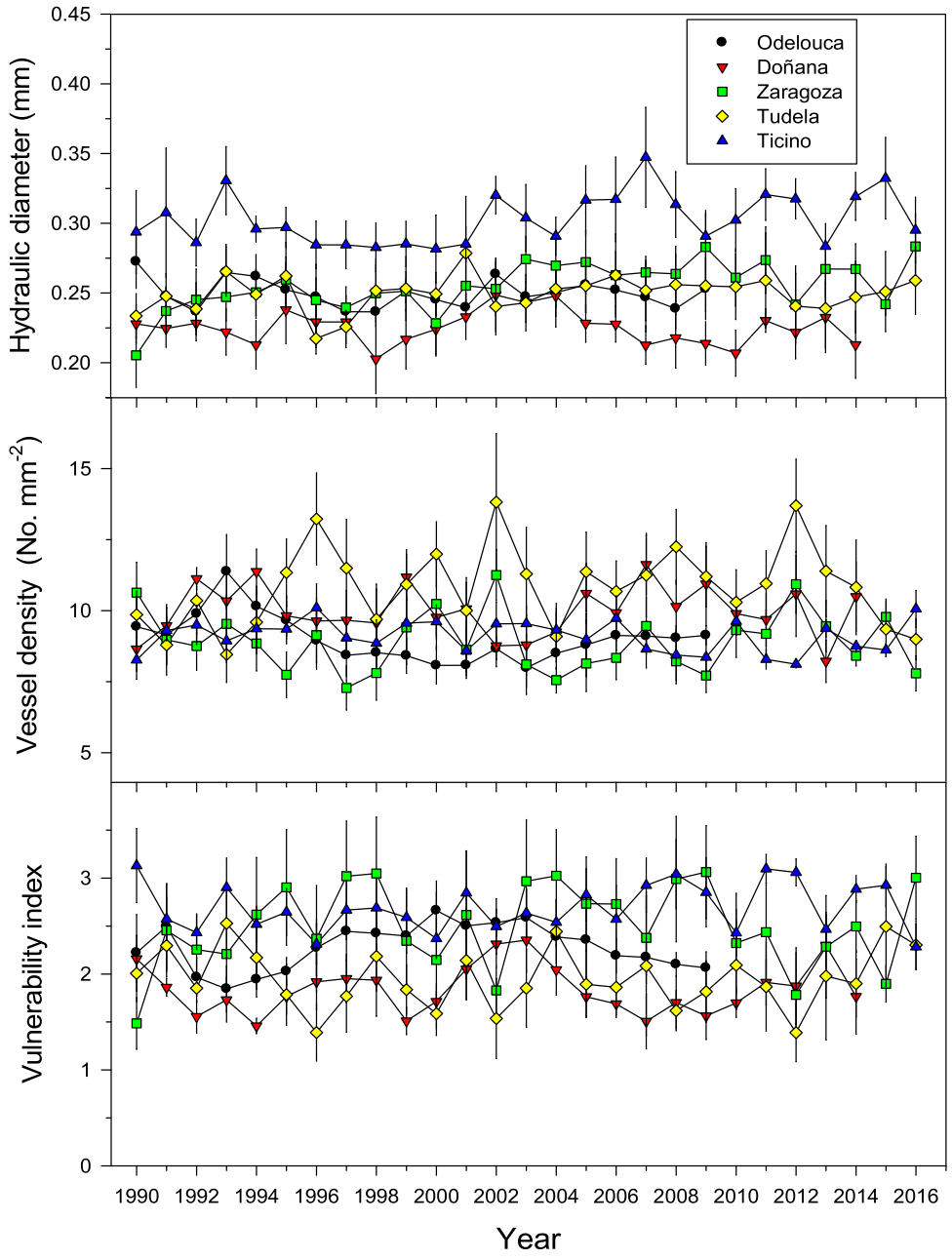

Fig. 2. Mean series of earlywood anatomical variables (*Dh*, hydraulic diameter; *VD*, vessel density; *VI*, vulnerability index). Values are means ± SE.

2.7. Statistical analyses

All statistical analyses were implemented in R (R Core Team, 2021). Growth data (TRW) were regressed against *Dh* for each site, and also considering the whole dataset, i.e. the 25 trees with EW anatomy data, using ordinary least square regressions. We also calculated a linear regression between TRW and *Dh* residuals after removing the effects of age on both variables in those 25 trees. This was achieved by fitting linear regressions and keeping the residuals.

Pearson correlation matrix was adopted to inspect for correlations among site-specific variables TRW; RWI, *Dh*, *VD*, and *VI*. The within-site coherence of these series was also assessed as the percentage of variance accounted for by the first principal component (PC1) of a Principal Component Analysis. Then, we related RWI and EW anatomy chronologies to yearly, seasonal or monthly climate (precipitation, mean temperature, water balance) and river flow data (only in Tudela and Zaragoza sites) using Pearson correlations. These correlations were calculated for the best-replicated period 1990–2016 for all sites excepting Doñana (1990–2014) and Odelouca (1990–2009). Previous analyses based on the same common period (1990–2009) for all sites produced similar results as those presented here. Anatomy variables were detrended by fitting linear regressions to mean site series and keeping residuals. However, correlations of wood anatomy residuals with climate or flow data were similar to those obtained with raw data so we present the later. Neither climate nor flow data were detrended since most variables did not present significant slopes for the period 1990–2016 excepting April, November and December temperature in Ticino and March, April and October P–PET and February-March flow data in Zaragoza and Tudela, which showed positive trends ($p < 0.01$). Analyses were performed from the previous September of the year

before the tree-ring was formed to September of the year of tree-ring formation. Correlations were calculated using the *treeclim* R package (Zang and Biondi, 2015). The RWI time series were also related to precipitation of the hydrological year (from prior October to current September) over the period 1990–2016 using ordinary least square regressions to assess the growth sensitivity on accumulated precipitation.

In the case of correlations involving monthly river flow data, we used Spearman rank correlations (r_s) since these data did not follow a normal distribution. Correlations between precipitation of the hydrological year and RWI are reported with their corresponding significance levels, and correlations based on monthly or seasonal data are presented indicating the 0.05 and 0.01 significance thresholds.

Linear mixed effects models (LMMs; Pinheiro and Bates, 2000) were fitted to investigate the relationships between earlywood *Dh* and seasonal climate variables (i.e., average temperature and summed P–PET) at the individual tree scale. In particular, seasonal temperature and P–PET of the previous autumn (son, September to November) and winter (dJF, previous December up to current February), and the current spring (MAM, March to May) and summer (JJA, June to August) were considered fixed effects, and individual trees were considered as random effects to account for repeated measures within each site. To account for the size- and age-related changes in tree growth, tree Dbh and age were incorporated as fixed effects. We also included a first order autocorrelation structure (AR1) to account for the dependency of *Dh* measures among consecutive years. The most parsimonious models were selected starting with a saturated model that contains all fixed explanatory variables. Fixed terms were centered to prevent collinearity between main effects and increase parameter interpretability (Schielzeth, 2010). The parameters of fixed structure in the equations were estimated by maximum likelihood (ML), whilst the restricted maximum likelihood (REML) was used to estimate the random components of the model using the *nlme* R library (Pinheiro et al., 2020). We used a stepwise search strategy using stepAIC from the *MASS* package (Venables and Ripley, 2002) to find the reduced model minimizing the AIC (Burnham and Anderson, 2002). The variance inflation factor (VIF) was computed on the reduced models in order to test collinearity: the threshold for rejecting alternatives was 2 since VIF > 2 suggests redundant explanatory variables (Dormann et al., 2013). Finally, we obtained the marginal (R^2_m) and conditional R^2 values (R^2_c), accounting for the variance explained by fixed and fixed plus random effects, respectively (Nakagawa and Schielzeth, 2013), using the *MuMIn* R package (Barton, 2020).

3. Results

3.1. Associations between growth and wood-anatomical variables

The TRW decreased as tree age increased ($r = -0.46$, $p = 0.019$). The VD decreased ($r = -0.41$, $p = 0.044$) and *VI* increased ($r = 0.47$, $p = 0.017$) as TRW increased, but neither *VD* nor *VI* were related to tree age.

At the individual level and considering all sites and mean values ($n = 25$ trees), the *Dh* accounted for 72% of the variance in growth rate (TRW) being both variables positively associated (Fig. 3). This positive relationship was also found when relating the residuals of *Dh* and TRW after correcting for age effects (Fig. S3). Within each site, *Dh* accounted for more than 50% explained variance in TRW ($n = 5$ trees per site), excepting in Odelouca (34%).

The coherence of mean RWI series within each site (mean correlation and mean percentage of variance accounted for by PC1) was much higher (e.g., TRW, 0.41 and 52.9%; RWI, 0.52 and 57.3%) than considering earlywood anatomical series (e.g., *Dh*, 0.15 and 44.0%; *VD*, 0.26 and 47.4%; Table S1). The Zaragoza site showed high within-site correlations for both growth (RWI, 0.66 and 69.8%) and anatomy (*Dh*, 0.36 and 51.6%) suggesting a high sensitivity to climate or river flow.

The *Dh*-TRW positive association observed for mean individual values was not detected when considering annual ring-width indices

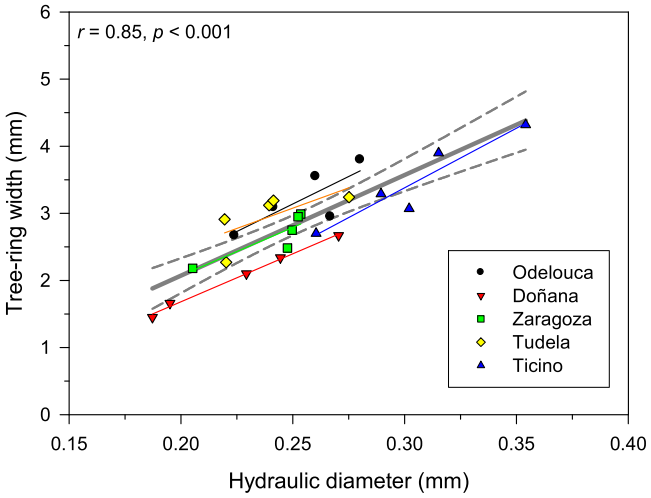

Fig. 3. Linear relationship between the mean tree values of earlywood hydraulic diameter (*Dh*) and tree-ring width. The different symbols and color lines (linear regression for each site) correspond to the five study sites. The continuous and dashed gray lines show the linear regression for all data and its 95% confidence intervals. The statistics show that the relationship is positive and highly significant considering all sites. (For interpretation of the references to color in this figure legend, the reader is referred to the web version of this article.)

(RWI) and *Dh* values, excepting in Zaragoza (Table 3). As expected, *Dh* and *VD* were negatively associated in all sites, whilst RWI and *VD* were negatively related in Doñana, Zaragoza and Tudela sites. Consequently, RWI and *VI* were positively related in these three sites.

When sites are compared, the RWI, *Dh* and *VD* series of the Zaragoza and Tudela nearby sites showed positive correlations (Table 3). The two warmest sites from south-western Iberia (Odelouca and Doñana) also presented positive correlations between their mean RWI and *VI* series. Lastly, the two most geographically distant sites (Odelouca and Ticino) showed a negative association between their RWI series indicating contrasting high-frequency growth variability.

3.2. Growth and wood anatomy responses to climate at site scale

Ash growth was improved by wet conditions as shown by the positive and significant ($p < 0.05$) relationships between precipitation of the hydrological year and annual RWIs found in all sites (Fig. 4, Table 4). Precipitation of the hydrological year explained 28–46%, 16% and 10% of the RWI variance in the warmest (Odelouca and Doñana), the wet-cool (Ticino) and the dry-continental (Tudela, Zaragoza) sites, respectively. The slopes of the fitted linear regressions were high and low in Zaragoza and Ticino, respectively, but they did not significantly differ ($F = 2.89$, $p = 0.09$).

Regarding wood anatomy data, *Dh* increased in response to prior October wet conditions in Odelouca, Tudela and Zaragoza (Fig. 5). The *Dh* also increased in response to wet February conditions in Zaragoza. Dry early summer conditions were associated to low *Dh* values in Tudela and Zaragoza. Lastly, *Dh* increased in response to warmer conditions from prior autumn to current spring in Ticino.

In Odelouca and Doñana sites, *VD* increased in response to cool conditions from prior autumn and winter up to summer (Fig. S4). In Tudela and Zaragoza, wet conditions in the prior autumn and winter, respectively, lead to decreased *VD*. In the case of the *VI*, wet-warm conditions in the prior autumn and winter increased it in Odelouca and Doñana (Fig. S5). In Tudela, a wet autumn was related to higher *VI* values and in Zaragoza this occurred during wet winters. In Ticino *VI* tended to increase in response to a dry prior autumn and warm winter-spring conditions.

Table 3
Significant relationships observed (a) between radial growth (RWI, ring-width index) and earlywood anatomy variables (*Dh*, hydraulic diameter; *VD*, vessel density; *VI*, vulnerability index), and (b) between sites' series of variables. The values are Pearson correlations and their significance levels are indicated by asterisks (*$p < 0.05$; **$p < 0.01$; ***$p < 0.001$).

(a) Correlations between variables				
Odelouca	Dh–VD, −0.465*			
Doñana	Dh–VD, −0.568**	RWI–VD, −0.696***	RWI–VI, 0.590**	
Zaragoza	Dh–VD, −0.542**	RWI–VD, −0.850***	RWI–VI, 0.749***	RWI–Dh, 0.454*
Tudela	Dh–VD, −0.420*	RWI–VD, −0.701***	RWI–VI, 0.747***	
Ticino	Dh–VD, −0.391*			
(b) Correlations between sites				
RWI	Zaragoza–Tudela, 0.551**	Odelouca–Doñana, 0.642**	Odelouca–Ticino, −0.459*	
Dh	Zaragoza–Tudela, 0.444*			
VD	Zaragoza–Tudela, 0.385*			
VI	Odelouca–Doñana, 0.590**			

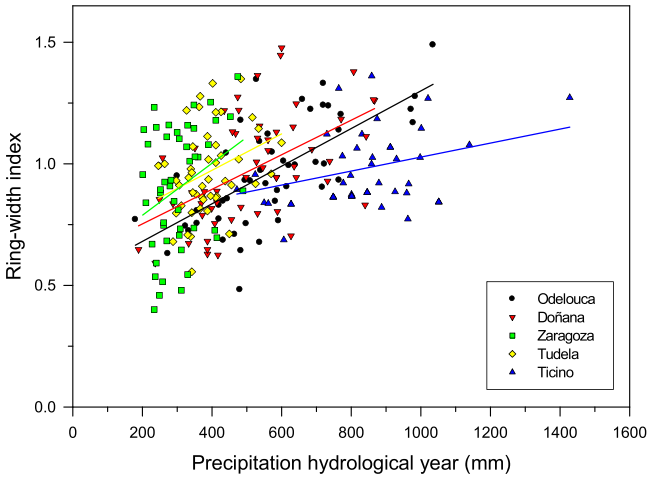

Fig. 4. Positive relationships observed between the precipitation of the hydrological year (from prior October to current September) and the ash ring-width index (RWI) in the five study sites. See statistics of the plotted regressions in Table 4.

Table 4
Statistics of the linear regressions fitted between the precipitation of the hydrological year and the mean site series of ring-width indices. The slope standard errors (SE) are presented.

Site	Slope (SE)	Intercept	*r*	R^2 (%)	*p*
Odelouca	0.00077 (0.00012)	0.52622	0.68	45.71	< 0.001
Doñana	0.00071 (0.00016)	0.61074	0.53	27.94	< 0.001
Zaragoza	0.00107 (0.00049)	0.57451	0.31	9.50	0.035
Tudela	0.00077 (0.00033)	0.67398	0.32	10.47	0.028
Ticino	0.00033 (0.00012)	0.68320	0.34	14.03	0.009

3.3. Relationships between growth, wood anatomy and river flow

Elevated river flow values in February, March and spring were positively related to *Dh* in Zaragoza, whilst high flow values in the prior November and winter and in January were inversely related to *VD* (Fig. 6). In Tudela, high flow values in March were also associated to large *Dh*, but not significantly.

3.4. Growth and wood anatomy responses to climate at the individual tree scale

At the individual level, we found similar relationships with *Dh* as at the site scale such as negative associations with summer water balance in Zaragoza an Tudela (Table 5). We also observed positive associations between *Dh* and tree Dbh in Ticino and Tudela. Wet conditions in the prior autumn and the current spring enhanced *Dh* in Tudela and Ticino, respectively, but the autumn effect was opposite in Zaragoza. Warm summer conditions were associated to low *Dh* values in Tudela. The low R^2_m values (on average 14%) evidenced that the models accounted for a low amount of variance explained by fixed effects, and the high R^2_c values (on average 57%) indicated that the amount of variance explained by fixed plus random effects was elevated.

4. Discussion

The growth and earlywood anatomy of ash under Mediterranean conditions responded to changes in local climate conditions and river flow, but responses greatly changed across the considered geographical and environmental gradients. As hypothesized, we found the largest ash *Dh* values in the wettest-coolest site (Ticino), where *Dh* increased in warm prior autumn-winter and current spring conditions. Ash growth rates were the least responsive to hydrological year precipitation in that wet site (lowest slope of all sites), whereas Zaragoza was the most responsive site showing the steepest slope (Fig. 3). Interestingly, ash growth rate covaried with earlywood *Dh*, which accounts for the potential hydraulic conductivity of the ring (Scholz et al., 2013). Here, we found that trees with wider earlywood vessels showed larger stemwood production, regardless their age. In one of the two sites with river flow data (Zaragoza), high spring flow peaks were associated to wider vessels and higher *Dh* values and a lower vessel density. In this dry-continental site, river flow explained less growth (RWI) variance than in the other site with similar climate conditions (Tudela). This difference suggests that ash earlywood anatomy has an intrinsic value as proxy of river flow fluctuations, which may show different responses than tree-ring width. The low percentage of ash growth-rate (RWI) variability explained by precipitation of the hydrological year in the sites located in the Middle Ebro basin (Tudela and Zaragoza) indicated that hydrological dynamics could account for part of the remaining unexplained growth variance (Rodríguez-González et al., 2021). In addition, these authors showed that winter precipitation and spring temperature are the strongest predictors of ash growth in these two sites.

Our findings partially agree with prior studies on these riparian forests since we previously found that ash growth increased with warmer conditions in two out of the five study sites (Rodríguez-González et al., 2021). In temperate floodplain *Quercus robur* forests, growth increased in response to warmer conditions, whereas a reduction in vessel size was observed in response to wet conditions (Tumajer and Treml, 2016). We found negative correlations of EW and *Dh* to wetness (P–PET) from June onwards, when leaf unfolding and EW vessel formation are completed (Hidalgo-Galvez et al., 2018; Gričar et al., 2020), suggesting carryover effects of EW on latewood production or dry winters followed by wet summers. In the case of *F. excelsior* growth was constrained by warm and dry conditions during the growing season (Roibu et al., 2020), which agrees with responses of *F. angustifolia* (Rodríguez-González et al., 2021). Ash species form shallow root systems making them very sensitive to reduced soil moisture and decreased groundwater levels with negative impact on carbon uptake and growth

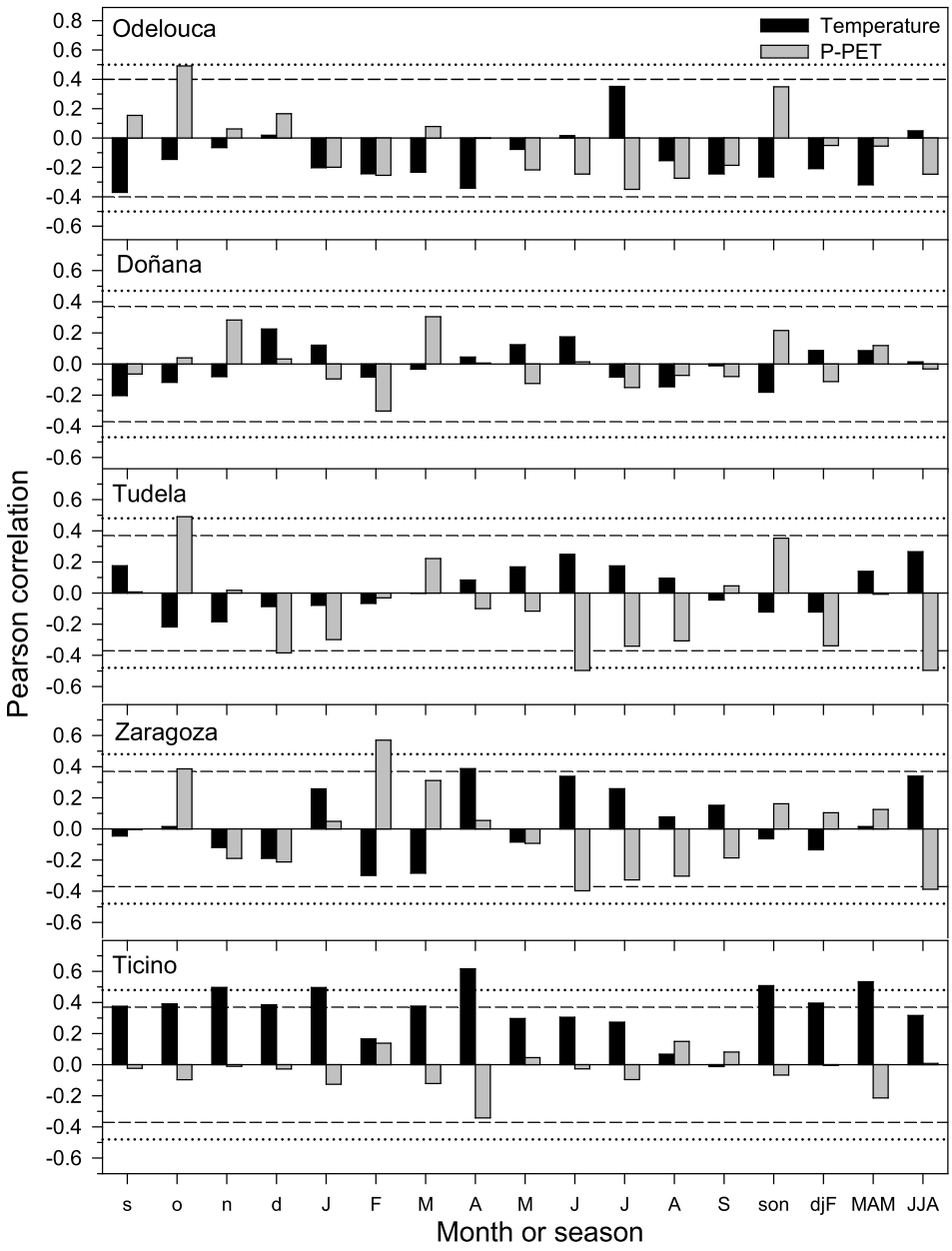

Fig. 5. Relationships between climate variables (mean temperature and water balance given by P–PET) and the mean series of earlywood hydraulic diameter (*Dh*) for the five ash study sites. Horizontal dashed and dotted lines indicate the 0.05 and 0.01 significance levels, respectively.

(Kerr and Cahalan, 2004). For instance, in a Mediterranean riparian forest, ash transpiration was constrained by low soil water contents (Nadal-Sala et al., 2017).

The rate of growth increment as precipitation increased was the highest in the Zaragoza dry-continental site indicating a higher responsiveness to precipitation, despite the precipitation-RWI slope was indistinguishable from the other sites (Table 4). This elevated growth responsiveness to precipitation and the sensitivity of *Dh* to changes in spring flow illustrate the relevance of climate variability and fluvial dynamics to explain ash productivity in that site. The growth coupling with local precipitation suggests a dependence of ash growth on the replenishment of shallow soil water reserves before growth onset, whilst groundwater variations could play a minor role (Dufour and Piégay, 2008). In the other nearby site from the Ebro basin (Tudela), growth rates responded more to river flow variability, suggesting that trees are more coupled with the river hydrological regime there than in Zaragoza, where land-use impacts are widespread (agricultural conversion, dam and dike building; cf. Ollero, 1990). The observed growth-flow couplings agree with the more mature status of Tudela floodplain forests (Ayerra, 1988). These results also agree with a study from central Spain where ash growth was favored by spring-summer river flows (González Muñoz et al., 2015). Finally, we are aware that local factors such as tree-to-tree competition, microtopography, soil depth or distance to the active river channel could also account for part of the unexplained growth and wood-anatomy variability at the individual level by affecting soil water availability and cell turgor during earlywood formation (Rodríguez-González et al., 2017).

Earlywood vessel formation depends on nutrients and assimilates stored before cambial division (Bréda and Granier, 1996), and vessel enlargement depends on both osmotic (nutrients/assimilates) and water potential (Cabon et al., 2020). Several studies on ring-porous broadleaf species found positive associations between late-winter and early-spring

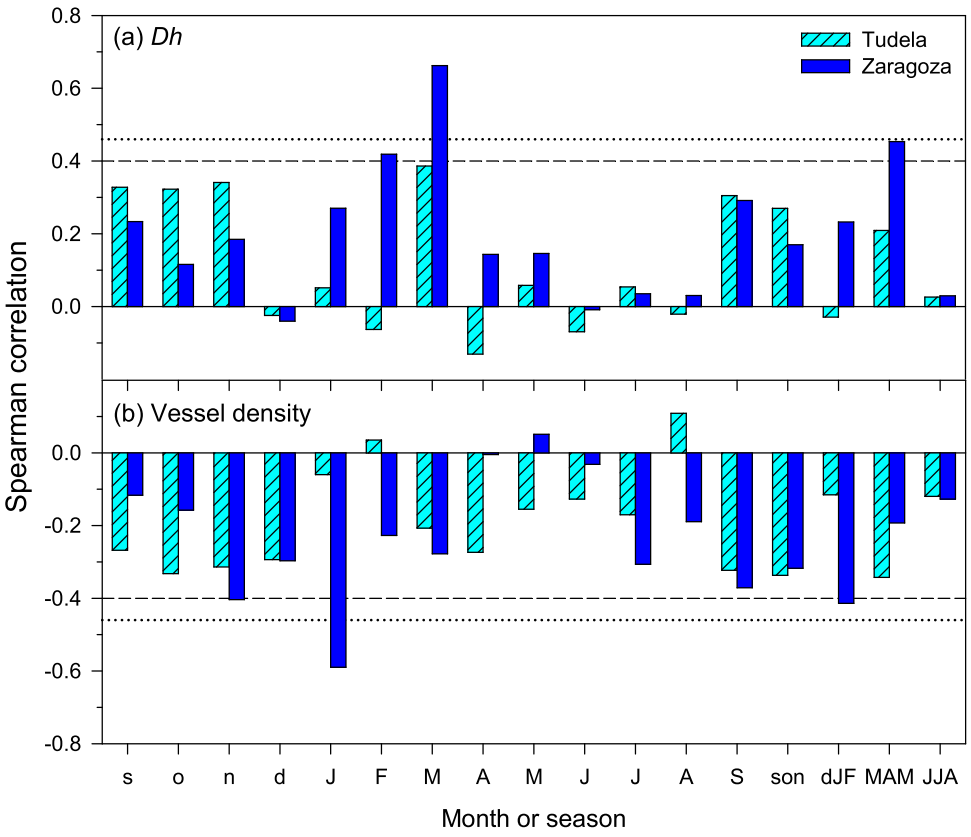

Fig. 6. Relationships between river flow and earlywood anatomy variables (a, *Dh*, hydraulic diameter; b, *VD*, vessel density) in the two sites located in the Ebro basin (Tudela and Zaragoza). Bars show Spearman correlation coefficients calculated between seasonal and monthly climate variables (mean temperature and total precipitation) and mean site series of earlywood anatomical data. Correlations were calculated from prior to current September (months abbreviated by lowercase letters correspond to the year prior to tree-ring formation). Horizontal dashed and dotted lines show the 0.05 and 0.01 significance levels, respectively.

Table 5
Standardized estimates of the selected linear mixed-effects models fitted to ash earlywood hydraulic diameter (*Dh*) as a function of seasonal climate variables (i.e., average temperature and water balance, P–PET), tree age and diameter at breast height (Dbh) in the five study sites. Numbers within parentheses are the standard errors of the standardized estimates. Previous and current-year months are abbreviated with lowercase and uppercase letters, respectively. Seasons are abbreviated as follows: son, previous autumn (son, September to November); winter (dJF, previous December up to current February); and current spring (MAM, March to May) and summer (JJA, June to August). The last two rows show the statistics of the models including the R^2_m and R^2_c, which correspond to the marginal and conditional R^2 values accounting for the variance explained by fixed and fixed plus random effects, respectively, and the Akaike Information Criterion (AIC). Significance levels: $^*p \leq 0.05$, $^{**}p < 0.01$, $^{***}p < 0.001$.

Climate variable	Season	Odelouca	Doñana	Tudela	Zaragoza	Ticino
Temperature	son					
	dJF	−0.16 (0.09)				
	MAM		0.11 (0.07)	0.08 (0.05)		
	JJA			−0.15** (0.07)		
P–PET	son			0.17***(0.04)	−0.15** (0.05)	
	dJF		−0.09 (0.06)		0.07 (0.04)	
	MAM		0.12 (0.07)			0.16*(0.07)
	JJA			−0.24***(0.07)	−0.10*(0.04)	
Age		−0.32*(0.15)	−0.18 (0.11)	−0.06 (0.13)	0.19 (0.21)	
Dbh		0.33 (0.24)		0.58***(0.17)	0.17 (0.37)	0.48***(0.12)
Age*Dbh		−0.25 (0.14)		0.26***(0.07)	−0.15***(0.04)	
R^2_m/R^2_c		0.12/0.32	0.04/0.64	0.14/0.78	0.13/0.79	0.28/0.34
AIC		917.25	1167.39	1221.40	1218.22	1381.27

temperature and earlywood vessel lumen area or *Dh* (e.g., González and Eckstein, 2003; Fonti et al., 2007; Alla and Camarero, 2012), which are in line with our results in the wettest-coolest Ticino site. Some studies carried out in dry areas also found positive influences of prior winter precipitation on earlywood vessel area in oak species such as *Quercus brantii* (Arsalani et al., 2018), which agree with our findings of positive associations between *Dh* and prior autumn-winter water availability in Odelouca, Tudela and Zaragoza warm or dry sites. This is also supported by the positive relationship between the growing-season precipitation prior to ring formation and *Dh* found in *Fraxinus nigra* (Tardif, 1996), *F. excelsior* (Klesse et al., 2020), and *Quercus alba* and *Quercus rubra* (Tardif and Conciatori, 2006). In mesic *Quercus petraea* sites, dry springs lead to the formation of rings with wider vessels (Martínez-Sancho et al., 2017). However, dry early summer conditions were associated to low *Dh* values in Tudela and Zaragoza ash stands in agreement with studies on Mediterranean ring-porous oaks from dry sites (e.g., *Quercus faginea*) where dry conditions are associated to the formation of vessels with small lumen area (Corcuera et al., 2004). This would suggest that some EW vessels are still formed in June and afterwards, which is not supported by phenology or xylogenesis studies (Gričar et al., 2020), or that we are detecting indirect effects of early-summer dry conditions on large vessels corresponding to the early latewood. Overall, our results on

earlywood anatomy evidence that a variable as *Dh* is sensitive to climate and river-flow variability. In contrast, vessel density showed mixed responses: as expected it decreased in response to prior wet conditions in Tudela and Zaragoza, which induce the formation of vessels with large lumen, but increased in response to prior cool conditions in Odelouca and Doñana leading to a decrease in the *VI*. The ability of the *VI* to discriminate sites as a function of wood anatomy ecological responses to climate, as Carlquist (1977) proposed, was limited with Ticino showing the highest *VI* values corresponding to more mesic conditions, and Doñana and Tudela showing the lowest *VI* values corresponding to xeric conditions. The high *VI* values in the dry-continental Zaragoza site could reflect wood-anatomical responses to river flow alteration characterized by higher water levels in winter and spring. Lastly, a positive relationship between *Dh* and growth rates agrees with another study on Manchurian ash (*Fraxinus mandshurica*) wet-cool sites across northeastern China, where ring-width was positively correlated with mean vessel area and *Dh* (Zhu et al., 2020); but, tree age could also play a major role in that case by explaining associations between growth rate and vessel size.

Our results should be interpreted with great caution since the wood anatomy chronologies do not meet dendrochronological standards regarding internal coherence, excepting in the Zaragoza site (Table S1). In addition, the LMMs fitted to *Dh* showed that most variance was due to random effects. The common signal of earlywood anatomical variables is usually much lower than for ring width (García-González et al., 2016), but earlywood anatomical series also contain environmental signals.

We found that increased aridification negatively impacts ash growth in warm-dry stands, despite warmer conditions could increase productivity in wet sites. The reduction of regular floods could lead to an overmature state of some of these ash forests benefiting ash in the short term, but leading to a long-term decline of the species in the more shaded and dense sites where invasive species such as black locust can establish or ash pathogen attacks become more common (González Muñoz et al., 2015; Janík et al., 2016; Adamcikova et al., 2018; Colangelo et al., 2018). The decline could be aggravated by more frequent and severe climatic and hydrological droughts, particularly in the current scenario of more regulated but also lower river flows than in the past (Stella and Bendix, 2019).

The information generated in this study can aid to assess the impacts of multiple stressors on drought-prone riparian forests and contribute to their conservation (Johnson et al., 2020). First, sharp changes in growth and wood anatomy in riparian ash forests ecosystems can be used as early-warning signals of vulnerability to drought or reduced river flow. Second, significant deviations of growth-anatomy covariation can also indicate stressing environmental conditions. Such deviations could be also used as early-warning signals to alleviate stress by reducing tree density or improving soil moisture levels through restoration and management of riparian ash forests.

5. Conclusions

Radial growth and potential hydraulic conductivity, inferred from changes tree-ring width and *Dh* changes, are impacted by climate variability and changes in river flow in riparian ash forests. Fast-growing trees produced wider earlywood vessels (higher *Dh*) showing a covariation between growth potential along with efficient water transport. Higher precipitation or river flow enhanced growth in all sites, albeit with low sensitivity in the wettest site. Earlywood vessels showed a larger lumen in response to wet conditions during prior autumn and winter, before cambial onset or in response to high river flow levels in late winter and early spring in the case of dry-continental sites. Conserving of drought-prone riparian ash forests will benefit from a better understanding of the long-term associations between growth, wood anatomy, climate, and river dynamics. The growth sensitivity to climate, and particularly water availability, of similar ash riparian forests subjected to seasonal drought makes them potentially vulnerable to severe climatic and hydrological droughts.

Declaration of Competing Interest

The authors declare that they have no known competing financial interests or personal relationships that could have appeared to influence the work reported in this paper.

Acknowledgment

We thank the comments provided by several reviewers. We are grateful to Antonio Albuquerque for field design, sampling and lab help in Doñana and Odelouca sites and Inês Marques and Rui Rivaes for help during sampling in Odelouca site. We thank the Doñana Biological Reserve and Doñana Biological Station, especially Ricardo Díaz Delgado. We also acknowledge the "Ticino Regional Park" administration for permission and Fulvo Caronni for logistic and field samplings support. This study was partially supported by the BBVA Foundation (SEDIBER project). PMRG was supported by Portuguese Foundation for Science and Technology (FCT), through CEEC Individual program grant number 2020.03356.CEECIND, and Forest Research Centre is a research unit funded by FCT (UIDB/00239/2020). Field sampling in Odelouca site was supported by RIPFLOW project (IWRM ERA-net Programme), and in Doñana by the "Programa de Acceso a la Infraestructura Científica y Tecnológica Singular" (ICTS-25-2010), project "Doñana wetland forests as sentinels of global change". This study was conducted with support of STSM 40285 "Long-term growth and functioning of a major tree species in Mediterranean floodplain forests" to M. Colangelo, funded by COST Action (CA16208) – CONVERGES: Knowledge Conversion for Enhancing Management of European Riparian Ecosystems and Services.

Appendix A. Supporting information

Supplementary data associated with this article can be found in the online version at doi:10.1016/j.dendro.2021.125891.

References

Adamcikova, K., Pažitný, J., Pastirčáková, K., 2018. Individual resistance of Fraxinus angustifolia and F. excelsior clones to Hymenoscyphus fraxineus. J. Plant. Prot. Res. 58, 227–233.

Alla, A.Q., Camarero, J.J., 2012. Contrasting responses of radial growth and wood anatomy to climate in a Mediterranean ring-porous oak, implications for its future persistence or why the variance matters more than the mean. Eur. J. For. Res. 131, 1537–1550.

Andersen, D., 2016. Climate, streamflow, and legacy effects on growth of riparian Populus angustifolia in the arid San Luis Valley. Colorado. J. Arid Environ. 134, 104–121.

Arsalani, M., Bräuning, A., Pourtahmasi, K., Azizi, G., Mohammadi, H., 2018. Multiple tree-ring parameters of Quercus brantii Lindel in SW Iran show a strong potential for intra-annual climate reconstruction. Trees Struct. Funct. 32, 1531–1546.

Ayerra, E., 1988. Los sotos de la ribera Tudelana. Servicio de Medio Ambiente del Gobierno de Navarra, Pamplona, Spain.

Barton, K., 2020. MuMIn: Multi-model inference. R package version 1.43.17. Retrieved from ⟨http://CRAN.R-project.org/package=MuMIn⟩.

Burnham, K.P., Anderson, D.R., 2002. Model Selection and Multimodel Inference: A Practical Information-Theoretic Approach. Springer, New York, USA.

Bréda, N., Granier, A., 1996. Intra- and interannual variations of transpiration, leaf area index and radial growth of a sessile oak stand (Quercus petraea). Ann. For. Sci. 53, 521–536.

Bunn, A., 2010. Statistical and visual crossdating in R using the dplR library. Dendrochronologia 28, 251–258.

Bunn, A., Korpela, M., Biondi, F., Campelo, F., Mérian, P., Qeadan, F., Zang, C., Puchacofrep, D., Wernicke, J., 2018. dplR, Dendrochronology Program Library in R. package version 1.42.1. ⟨https://cran.r-project.org/web/packages/dplR/index.html⟩.

Cabon, A., Fernández-de-Uña, L., Gea-Izquierdo, G., Meinzer, F.C., Woodruff, D.R., Martínez-Vilalta, J., De Cáceres, M., 2020. Water potential control of turgor-driven tracheid enlargement in Scots pine at its xeric distribution edge. New Phytol. 225, 209–221.

Campelo, F., García-González, I., Nabais, C., 2012. detrendeR – A graphical user interface to process and visualize tree-ring data using R. Dendrochronologia 30, 57–60.

Carlquist, S., 1977. Ecological factors in wood evolution, a floristic approach. Am. J. Bot. 64, 887–896.

Caudullo, G., Houston Durrant, T., 2016. Fraxinus angustifolia in Europe, distribution, habitat, usage and threats. In: San-Miguel-Ayanz, J., de Rigo, D., Caudullo, G.,

Houston Durrant, T., Mauri, A. (Eds.), European Atlas of Forest Tree Species. Publ. Off. EU, Luxembourg, p. e0101d2.
Caudullo, G., Welk, E., San-Miguel-Ayanz, J., 2017. Chorological maps for the main European woody species. Data in Brief 12, 662–666.
Cochard, H., Peiffer, M., Le Gall, K., Granier, A., 1997. Developmental control of xylem hydraulic resistances and vulnerability to embolism in Fraxinus excelsior L, impacts on water relations. J. Exp. Bot. 48, 655–663.
Colangelo, M., Camarero, J.J., Ripullone, F., Gazol, A., Sánchez-Salguero, R., Oliva, J., Redondo, M.A., 2018. Drought decreases growth and increases mortality of coexisting native and introduced tree species in a temperate floodplain forest. Forests 9, 1–17.
Corcuera, L., Camarero, J.J., Gil-Pelegrín, E., 2004. Effects of a severe drought on growth and wood-anatomical properties of Quercus faginea. IAWA J. 25, 185–204.
Cornes, R., van der Schrier, G., van den Besselaar, E.J.M., Jones, P.D., 2018. An ensemble version of the E-OBS temperature and precipitation datasets. J. Geophys. Res. Atmos. 123, 9391–9409.
Dormann, C.F., Elith, J., Bacher, S., Buchmann, C., Carl, G., Carré, G., Marquéz, J.R.G., Gruber, B., Lafourcade, B., Leitão, P.J., Münkemüller, T., McClean, C., Osborne, P.E., Reineking, B., Schröder, B., Skidmore, A.K., Zurell, D., Lautenbach, S., 2013. Collinearity: a review of methods to deal with it and a simulation study evaluating their performance. Ecography 36, 27–46.
Dufour, S., Piégay, H., 2008. Geomorphological controls of Fraxinus excelsior growth and regeneration in floodplain forests. Ecology 89, 205–215.
Dufour, S., Rodríguez-González, P.M., Laslier, M., 2018. Tracing the scientific trajectory of riparian vegetation studies, Main topics, approaches and needs in a globally changing world. Sci. Tot. Environ. 653, 1168–1185.
Enderle, R., Stenlid, J., Vasaitis, R., 2019. An overview of ash (Fraxinus spp.) and the ash dieback disease in Europe. CAB Rev. 14, 1–12.
Fonti, P., Solomonoff, N., García- González, I., 2007. Earlywood vessels of Castanea sativa record temperature before their formation. New Phytol. 173, 562–570.
Fonti, P., von Arx, G., García-González, I., Eilmann, B., Sass-Klaassen, U., Gärtner, H., Eckstein, D., 2010. Studying global change through investigation of the plastic responses of xylem anatomy in tree rings. New Phytol. 185, 42–53.
Fritts, H.C., 1976. Tree Rings and Climate. Academic Press, London.
Frutos, L.M., Ollero, A., Sánchez Fabre, M., 2004. Caracterización del Ebro y su cuenca y variaciones en su comportamiento hidrológico. In: Gil Olcina, A. (Ed.), Alteración de los regímenes fluviales peninsulares, ed. .,. Fundación Cajamurcia, Murcia, Spain, pp. 233–280.
Funada, R., Catesson, A.M., 1991. Partial cell wall lysis and the resumption of meristematic activity in Fraxinus excelsior cambium. IAWA Bull. 12, 439–444.
García-González, I., Souto-Herrero, M., Campelo, F., 2016. Ring-porosity and earlywood vessels: a review on extracting environmental information through time. IAWA J. 37, 295–314.
Gärtner, H., Nievergelt, D., 2010. The core-microtome, a new tool for surface preparation on cores and time series analysis of varying cell para- meters. Dendrochronologia 28, 85–92.
Gomes Marques, I., Campelo, F., Rivaes, R., Albuquerque, A., Ferreira, M.T., Rodríguez-González, O., 2018. Tree rings reveal long-term changes in growth resilience in Southern European riparian forests. Dendrochronologia 52, 167–176.
González, I.G., Eckstein, D., 2003. Climatic signal of earlywood vessels of oak on a maritime site. Tree Physiol. 23, 497–504.
González Muñoz, N., Linares, J.C., Castro-Díez, P., Sass-Klaassen, U., 2015. Contrasting secondary growth and water use efficiency patterns in native and exotic trees co-occurring in inner Spain riparian forests. Forest Syst. 24, 017.
Gortan, E., Nardini, A., Gascó, A., Salleo, S., 2009. The hydraulic conductance of Fraxinus ornus leaves is constrained by soil water availability and coordinated with gas exchange rates. Tree Physiol. 29, 529–539.
Gričar, J., Vedenik, A., Skoberne, G., Hafner, P., Prislan, P., 2020. Timeline of leaf and cambial phenology in relation to development of initial conduits in xylem and phloem in three coexisting sub-Mediterranean deciduous tree species. Forests 11, 1104.
Hidalgo-Galvez, M.D., Garcia-Mozo, H., Oteros, J., Mestre, A., Botey, R., Galán, C., 2018. Phenological behaviour of early spring flowering trees in Spain in response to recent climate changes. Theor. Appl. Climatol. 132, 263–273.
Holmes, R., 1983. Computer-assisted quality control in tree-ring dating and measurement. Tree-Ring Bull. 43, 69–78.
Hultberg, T., Sandström, J., Felton, A., Öhman, K., Rönnberg, J., Witzell, J., Cleary, M., 2020. Ash dieback risks an extinction cascade. Biol. Conserv. 244, 108516.
Janík, D., Adam, D., Hort, L., Král, K., Šamonil, P., Unar, P., Vrška, T., 2016. Patterns of Fraxinus angustifolia in an alluvial old-growth forest after declines in flooding events. Eur. J. For. Res. 135, 215–228.
Johnson, M.F., Thorne, C.R., Castro, J.M., Kondolf, G.M., Mazzacano, C.S., Rood, S.B., Westbrook, C., 2020. Biomic river restoration, A new focus for river management. River Res. Appl. 36, 3–12.
Kerr, G., Cahalan, C., 2004. A review of site factors affecting the early growth of ash (*Fraxinus excelsior* L.). For. Ecol. Manag. 188, 225–234.
Klesse, S., von Arx, G., Gossner, M.M., Hug, C., Rigling, A., Queloz, V., 2020. Amplifying feedback loop between growth and wood anatomical characteristics of *Fraxinus excelsior* explains size-related susceptibility to ash dieback. Tree Physiol. 41, 683–696.
Manzano, M., Custodio, E., Mediavilla, C., Montes, C., 2005. Effects of localised intensive aquifer exploitation on the Doñana wetlands (SW Spain). In: Sahuquillo, A., Capilla, J., Martínez-Cortina, L., Sanchez Vila, X. (Eds.), Groundwater intensive use. International Association of Hydrogeologists, eds. Taylor & Francis, pp. 209–219.
Martínez-Sancho, E., Dorado-Liñán, I., Heinrich, I., Helle, G., Menzel, A., 2017. Xylem adjustment of sessile oak at its southern distribution limits. Tree Physiol. 37, 903–914.
Nadal-Sala, D., Sabaté, S., Sánchez-Costa, E., Poblador, S., Sabater, F., Gracia, C., 2017. Growth and water use performance of four co-occurring riparian tree species in a Mediterranean riparian forest. For. Ecol. Manag. 396, 132–142.
Nakagawa, S., Schielzeth, H., 2013. A general and simple method for obtaining R2 from generalized linear mixed-effects models. Methods Ecol. Evol. 4, 133–142.
Ollero, A., 1990. Espacios naturales de ribera en el municipio de Zaragoza. Geographicalia 27, 121–136.
Ollero, A., 2007. Channel adjustments, floodplain changes and riparian ecosystems of the middle Ebro River, assessment and management. Int. J. Water Res. Dev. 23, 73–90.
Olson, M.E., Soriano, D., Rosell, J.A., Anfodillo, T., Donoghue, M.J., Edwards, E.J., León-Gómez, C., Dawson, T., Camarero Martínez, J.J., Castorena, M., Echeverría, A., Espinosa, C.I., Fajardo, A., Gazol, A., Isnard, S., Lima, R.S., Marcati, C.R., Méndez-Alonzo, R., 2018. Plant height and hydraulic vulnerability to drought and cold. Proc. Natl. Acad. Sci. USA 115, 7551–7556.
Pinheiro, J.C., Bates, D.M., 2000. Mixed Effects Models in S and S-Plus. Springer, New York, USA.
European Environment Agency (EEA), 2015. Conservation status of habitat types and species (Article 17, Habitats Directive 92/43/EEC). ⟨https//www.eea.europa.eu/data-and-maps/daviz/conservation-status-of-floodplain-forest-habitats⟩ (Accessed 15 December 2020).
Pinheiro, J., Bates, D., DebRoy, S., Sarkar, D., R Core Team, 2020. nlme: Linear and Nonlinear Mixed Effects Models. R package version 3.1-152, ⟨https://CRAN.R-project.org/package=nlme⟩.
R Core Team, 2021. R, A language and environment for statistical computing. R Foundation for Statistical Computing, Vienna, Austria.
Rodríguez-González, P.M., Ferreira, M.T., Albuquerque, A., Espirito Santo, D., Ramil Rego, P., 2008. Spatial variation of wetland woods in the latitudinal transition to arid regions, a multiscale approach. J. Biogeogr. 35, 1498–1511.
Rodríguez-González, P.M., Stella, J.C., Campelo, F., Ferreira, M.T., Albuquerque, A., 2010. Subsidy or stress? Tree structure and growth in wetland forests along a hydrological gradient in Southern Europe. For. Ecol. Manag. 259, 2015–2025.
Rodríguez-González, P.M., Campelo, F., Albuquerque, A., Rivaes, R., Ferreira, T., Pereira, J.S., 2014. Sensitivity of black alder (*Alnus glutinosa* [L.] Gaertn.) growth to hydrological changes in wetland forests at the rear edge of the species distribution. Plant Ecol. 215, 233–245.
Rodríguez-González, P.M., Albuquerque, A., Martínez-Almarza, M., Díaz-Delgado, R., 2017. Long-term monitoring for conservation management: Lessons from a case study integrating remote sensing and field approaches in floodplain forests. J. Environ. Manag. 202, 392–402.
Rodríguez-González, P.M., Colangelo, M., Sánchez-Miranda, A., Sánchez-Salguero, R., Campelo, F., Rita, A., Gomes Marques, I., Albuquerque, A., Ripullone, F., Camarero, J.J., 2021. Climate, drought and hydrology drive narrow-leaved ash growth dynamics in southern European riparian forests. For. Ecol. Manag. 490, 119128.
Roibu, C.-C., Sfecla, V., Mursa, A., Ionita, M., Nagavciuc, V., Chiriloaei, F., Les, I., Popa, I., 2020. The climatic response of tree ring width components of ash (*Fraxinus excelsior* L.) and common oak (*Quercus robur* L.) from Eastern Europe. Forests 11, 600.
Schielzeth, H., 2010. Simple means to improve the interpretability of regression coefficients. Methods Ecol. Evol. 1, 103–113.
Schneider, C.A., Rasband, W.S., Eliceiri, K.W., 2012. NIH Image to ImageJ, 25 years of image analysis. Nat. Methods 9, 671–675.
Scholz, A., Klepsch, M., Karimi, Z., Jansen, S., 2013. How to quantify conduits in wood? Front. Plant Sci. 4, 56.
Schook, D.M., Friedman, J.M., Stricker, C.A., Csank, A.Z., Cooper, D.J., 2020. Short- and long-term responses of riparian cottonwoods (Populus spp.) to flow diversion: analysis of tree-ring radial growth and stable carbon isotopes. Sci. Total Environ. 735, 139523.
Scott, M.L., Shafroth, P.B., Auble, G.T., 1999. Responses of riparian cottonwoods to alluvial water table declines. Environ. Manag. 23, 347–358.
Singer, M.B., Stella, J.C., Dufour, S., Piégay, H., Wilson, R.J., Johnstone, L., 2013. Contrasting water uptake and growth responses to drought in co-occurring riparian tree species. Ecohydrology 6, 402–412.
Sperry, J.S., Nichols, K.L., Sullivan, J.E.M., Eastlack, S.E., 1994. Xylem embolism in ring-porous, diffuse-porous, and coniferous trees of Northern Utah and Interior Alaska. Ecology 75, 1736–1752.
Stella, J.C., Bendix, J., 2019. Multiple stressors in riparian ecosystems. In: Sabater, S., Elosegi, A., Ludwig, R. (Eds.), Multiple Stressors in River Ecosystems. Elsevier, pp. 81–110.
Stella, J.C., Riddle, J., Piegay, H., Gagnage, M., Tremelo, M.L., 2013a. Climate and local geomorphic interactions drive patterns of riparian forest decline along a Mediterranean Basin river. Geomorphology 202, 101–114.
Stella, J.C., Rodríguez-González, P.M., Dufour, S., Bendix, J., 2013b. Riparian vegetation research in Mediterranean-climate regions, common patterns, ecological processes, and considerations for management. Hydrobiologia 719, 291–315.
Tardif, J.C., 1996. Earlywood, latewood and total ring width of a ring-porous species (*Fraxinus nigra* Marsh.) in relation to climatic and hydrologic-factors. In: Dean, J.S., Meko, D.M., Swetnam, T.W. (Eds.), Tree Rings, Environment and Humanity. Radiocarbon, Tucson, pp. 315–324.
Tardif, J.C., Conciatori, F., 2006. Influence of climate on tree rings and vessel features in red oak and white oak growing near their northern distribution limit, southwestern Quebec, Canada. Can. J. For. Res. 36, 2317–2330.

Trabucco, A., Zomer, R., 2019. Global Aridity Index and Potential Evapotranspiration (ET0) Climate Database v2. Available at ⟨https//doi.org/10.6084/m9.figshare.7504448.v3⟩ (Accessed 16 December 2020).

Tumajer, J., Treml, V., 2016. Response of floodplain pedunculate oak (*Quercus robur* L.) tree-ring width and vessel anatomy to climatic trends and extreme hydroclimatic events. For. Ecol. Manag. 379, 185–194.

Utsumi, Y., Sano, Y., Funada, R., Fujikawa, S., Ohtani, J., 1999. The progression of cavitation in earlywood vessels of *Fraxinus mandshurica* var *japonic*a during freezing and thawing. Plant Physiol. 121, 897–904.

Valor, T., Camprodon, J., Buscarini, S., Casals, P., 2020. Drought-induced dieback of riparian black alder as revealed by tree rings and oxygen isotopes. For. Ecol. Manag. 478, 118500.

Venables, W.N., Ripley, B.D., 2002. Modern Applied Statistics with S. Springer, New York.

Wigley, T.M.L., Briffa, K.R., Jones, P.D., 1984. On the average value of correlated time series, with applications in Dendroclimatology and hydrometeorology. J. Clim. Appl. Meteorol. 23, 201–213.

Zang, C., Biondi, F., 2015. treeclim, an R package for the numerical calibration of proxy-climate relationships. Ecography 38, 431–436.

Zhu, L., Cooper, D.J., Yuan, D., Li, Z., Zhang, Y., Liang, H., Wang, X., 2020. Regional scale temperature rather than precipitation determines vessel features in earlywood of Manchurian ash in temperate forests. J. Geophys. Res. Biogeosci. 125 e2020JG005955.